



## OPEN ACCESS

## EDITED BY

Jan Heiland,  
Max Planck Society, Germany

## REVIEWED BY

Edgar O. Reséndiz-Flores,  
Tecnológico Nacional de México/IT  
Saltillo, Mexico  
Xiangyun Long,  
Hunan University, China

## \*CORRESPONDENCE

Jörg Fehr  
✉ joerg.fehr@itm.uni-stuttgart.de

RECEIVED 01 February 2023

ACCEPTED 03 April 2023

PUBLISHED 27 April 2023

## CITATION

Hay J, Schories L, Bayerschen E, Wimmer P,  
Zehbe O, Kirschbichler S and Fehr J (2023)  
Application of data-driven surrogate models for  
active human model response prediction and  
restraint system optimization.  
*Front. Appl. Math. Stat.* 9:1156785.  
doi: 10.3389/fams.2023.1156785

## COPYRIGHT

© 2023 Hay, Schories, Bayerschen, Wimmer,  
Zehbe, Kirschbichler and Fehr. This is an  
open-access article distributed under the terms  
of the [Creative Commons Attribution License  
\(CC BY\)](https://creativecommons.org/licenses/by/4.0/). The use, distribution or reproduction  
in other forums is permitted, provided the  
original author(s) and the copyright owner(s)  
are credited and that the original publication in  
this journal is cited, in accordance with  
accepted academic practice. No use,  
distribution or reproduction is permitted which  
does not comply with these terms.

# Application of data-driven surrogate models for active human model response prediction and restraint system optimization

Julian Hay<sup>1</sup>, Lars Schories<sup>1</sup>, Eric Bayerschen<sup>2</sup>, Peter Wimmer<sup>3</sup>,  
Oliver Zehbe<sup>3</sup>, Stefan Kirschbichler<sup>3</sup> and Jörg Fehr<sup>4\*</sup>

<sup>1</sup>Corporate Research and Development, ZF Friedrichshafen AG, Friedrichshafen, Germany, <sup>2</sup>Passive Safety Systems, ZF Friedrichshafen AG, Alfdorf, Germany, <sup>3</sup>Virtual Vehicle Research GmbH, Graz, Austria, <sup>4</sup>Institute of Engineering and Computational Mechanics, University of Stuttgart, Stuttgart, Germany

Surrogate models are a must-have in a scenario-based safety simulation framework to design optimally integrated safety systems for new mobility solutions. The objective of this study is the development of surrogate models for active human model responses under consideration of multiple sampling strategies. A Gaussian process regression is chosen for predicting injury values based on the collision scenario, the occupant's seating position after a pre-crash movement and selected restraint system parameters. The trained models are validated and assessed for each sampling method and the best-performing surrogate model is selected for restraint system parameter optimization.

## KEYWORDS

surrogate modeling, active human model, prediction of injury values, restraint system optimization, simulation framework

## 1. Introduction

With the invention of the automobile in 1889, Carl Benz ushered in a new age of mobility. Since then, vehicle and occupant safety has played an important role, resulting in various vehicle safety concepts, laws and regulations, each of which has reduced traffic accidents and fatalities, and today enables the concept Vision Zero [1] with no fatalities on the road. Nowadays it is much safer to enter a vehicle than it was 30 years ago (see Figure 1). Passive Safety devices like the belt or airbags decreased the fatalities on the road. Active vehicle safety functions include, for example, an adaptive cruise control (ACC) [3], a forward collision warning (FCW) and an autonomous emergency braking (AEB) [4]. In contrast to passive safety systems, active vehicle safety functions primarily act in the so-called pre-crash phase and aim to prevent collisions or mitigate collision consequences by reducing the impact speed, for example. Those systems act prior to an impact and therefore have much more possibilities to influence the crash outcome.

Integrated vehicle safety systems that combine active and passive safety components, called integrated vehicle safety—hold great promise for reducing the number and severity of traffic accidents [5]. Therefore, integrated safety is investigated in detail in various international research projects, e.g. the OSCCAR [6] and VIRTUAL [7] project. As specified in the Euro NCAP roadmap, future vehicle safety systems need to fulfill new requirements and perform robust in existing and future real-world driving scenarios. As a result, virtual

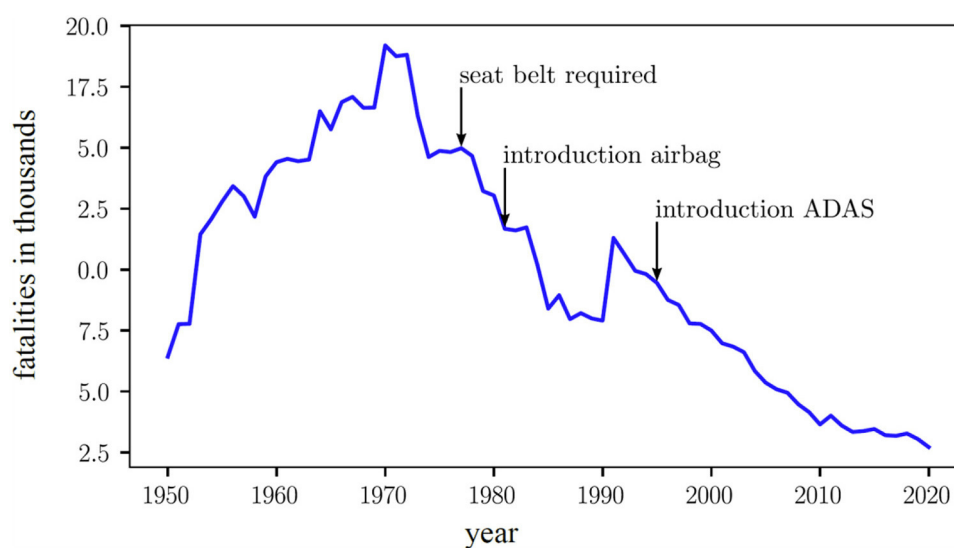


FIGURE 1

Fatalities on German roads since 1950 [2]. Detailed description of the data-flow in the simulation framework for scenario-based safety performance assessment, combining scenario, vehicle crash and occupant restraint system simulation. The arrows describe the in- and outputs to the specific simulator instances.

and simulative test methods [8] will become increasingly important in the future, as they offer a more efficient and cost-effective way to evaluate and optimize the performance of these systems. Often such an approach is called a holistic scenario-based analysis and safety performance assessment of novel integrated safety system solutions.

The differences in initial posture in the pre-crash phase can have an influence on the risk of injury during the in-crash phase [9]. Therefore, the pre-crash phase is so important, to consider for the design of holistic safety systems. A braking or steering maneuver may cause the occupant to experience lateral or longitudinal shifts and may not be seated in the default position when the collision occurs.

The proposed simulation framework (see Figure 2B) is an attempt to combine all relevant simulation steps from normal driving to safety-critical events (see Figures 2A, B) and [10]. The simulations should help accelerate and digitize the currently separated areas of active and passive vehicle safety system by using one common framework. The framework consists of three simulation entities.

The scenario simulation in Carmaker (Figure 2Ba) includes two vehicles, equipped with active safety systems, and provides the vehicle trajectory in the pre-crash phase as well as the resulting collision configuration. Subsequently, a FEM vehicle crash simulation in LS-Dyna (Figure 2Bb) is performed to calculate the crash pulse of the interior survival space. Finally, the acceleration signals from the pre- and in-crash phase are transferred to a Madymo vehicle interior model, including an active human model (AHM), which is positioned on the driver seat (Figure 2Bc) and for a chosen set of restraint system parameters the  $HIC_{36}$  and chest deflection are computed.

The computational cost of simulating passenger movement and injury prediction values using FEM and MBS simulations can be

very high. For example, the passenger movement simulation can take up to 3 h to simulate only 3 s of real-world time, and a single crash simulation can take up to 20 h on 10 CPUs to simulate only 180 ms of real-world time. Due to the enormous diversity in collision configurations and occupant behavior in real-world accidents, the number of considered scenarios and thus, the effort in simulation significantly increases, e.g., 300 scenarios with 3 active safety system variants result in  $900 \text{ FEM and MBS simulations}^1$   $900 \cdot 20 \text{ h} \approx 2 \text{ y CPU time}$ . These time requirements can make it challenging to perform scenario-based assessments of integrated vehicle safety systems with conventional simulation methods, as many simulations may be required to cover different scenarios and system configurations.

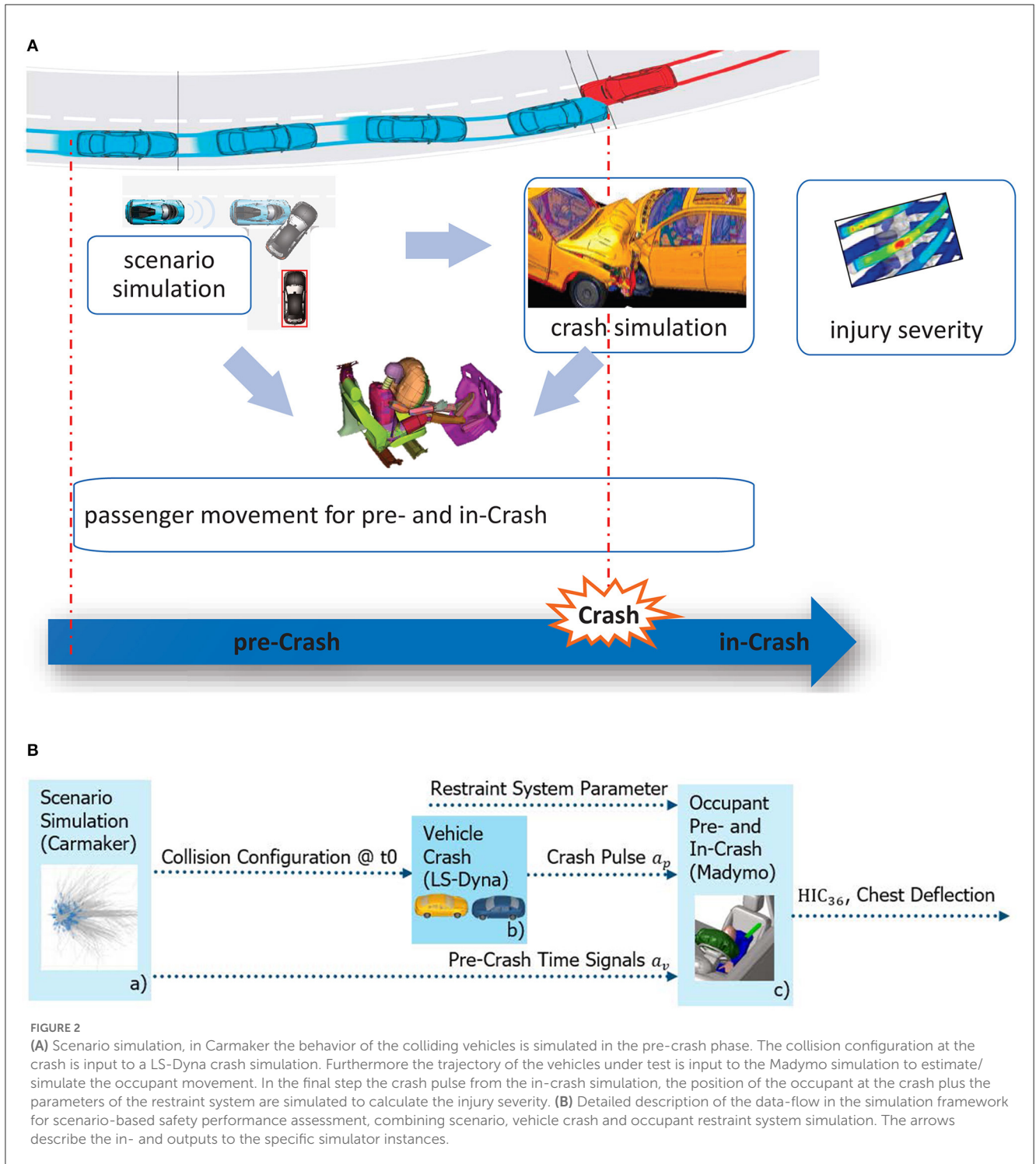
Since many of the simulation codes used in vehicle safety are proprietary and closed-source. Non-intrusive, data-based surrogate models are often the only possible choice. The final framework in Figure 3 used for an efficient approximation of the human body model response is then obtained by exchanging the FEM and MBS simulations for a suitable data-based surrogate model.

As shown in [11] the crash pulse of the FEM model of the crash can be predicted in a cost- and time-efficient manner by Gaussian Process Regression (GPR).

The paper has three primary foci:

1. The evaluation of the suitability of surrogate models for the prediction of the human body model response, i.e., the MBS simulation;
2. The tradeoff between the number of samples in the training and the accuracy of the data-driven surrogate models.

<sup>1</sup> One FE Simulation runs for approx 20 h on 10 CPUs to simulate 180 ms.

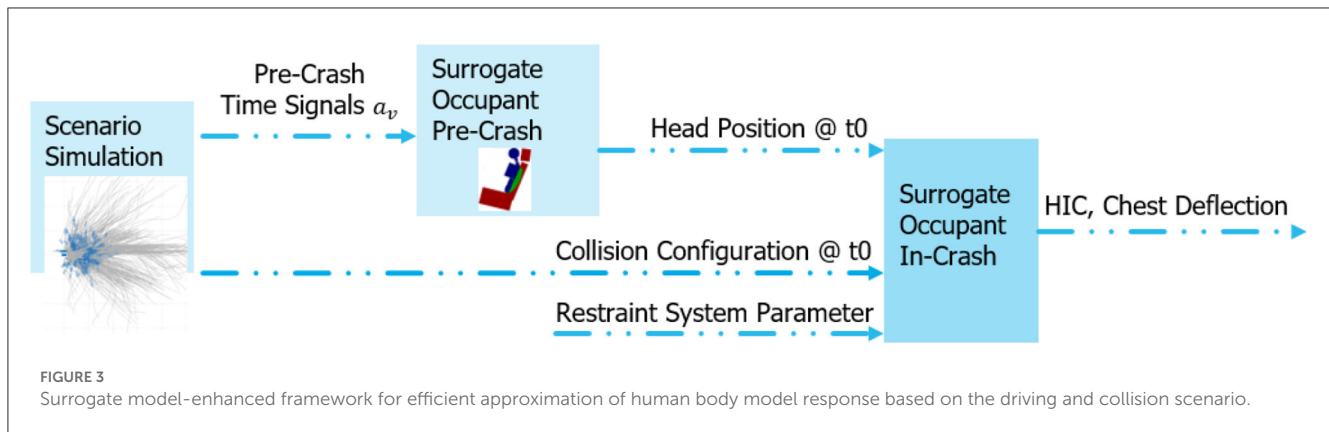


3. Can the developed surrogate models be applied for an efficient optimization of the restraint system parameters for a given scenario?

Other published studies on surrogate model development for human body model [12] response prediction in crash situations performed a variation of the restraint system parameter to predict the Life Years Lost [13] or varied the crash pulse and safety system usage [14]. In Berthelson et al. [15] a surrogate model selection algorithm was applied for HIC<sub>36</sub> prediction based on the collision configuration and found the GPR as best-suited surrogate model.

Similar to [11] a Gaussian process regression (GPR) model is used to learn the mapping from inputs to outputs. The concrete data set  $D: \mathbf{X} \rightarrow \mathbf{y}$  of the learning problem consists of the input values  $\mathbf{X} \in \mathbb{R}^9$ , which are the initial head position  $\mathbf{d}_{head}^{PC} \in \mathbb{R}^2$ , the collision configuration  $\mathbf{p}_{Collision} \in \mathbb{R}^3$ , and selected restraint system parameters  $\mathbf{p}_{Restraint} \in \mathbb{R}^4$ , and the output values  $\mathbf{y} = \{HIC_{36}, CD\} \in \mathbb{R}^2$ , i.e. the head injury criterion (HIC<sub>36</sub>) and chest deflection (CD).

Typically, the accuracy of data-driven surrogate models increases with the number of samples. As vehicle safety simulations



are rather expensive and time consuming, there exists a tradeoff between the size of the generated training set and the surrogate models' accuracy. The design of experiments addresses that conflict and provides multiple sampling methods that aim to cover the entire parameter space while maximizing the information gain. In this study, three sampling methods—a d-optimal design, a space-filling design and an adaptive sampling scheme—are compared and assessed regarding their suitability for surrogate model development for occupant safety.

In addition to a variation of restraint system parameter and the collision configuration, this study includes a variation of the occupant's posture resulting from the pre-crash scenario, which is in the simplest case represented by the head position  $\mathbf{d}_{head}^{PC} \in \mathbb{R}^2$ . The paper is structured in the following way. Section 2 explains the methods for the simulation framework, the considered sampling and training methods for data-based surrogate modeling, and the restraint system optimization process. Results with respect to surrogate model performance and restraint system optimization are presented in Section 3. The paper concludes with a discussion in Section 4.

## 2. Methods

The surrogate modeling process can be divided into three steps, training data generation, model training and validation. Since conventional vehicle safety system simulations, such as FEM and MBS, are computationally expensive, the training set should be as small as possible while ensuring broad coverage of the entire parameter space. In order to address this tradeoff, different sampling methods for selecting the training data are applied. Subsequently, the surrogate model is trained and validated with the generated data. Finally, the resulting models are compared with respect to performance on previously unseen data.

### 2.1. Simulation framework for training data generation

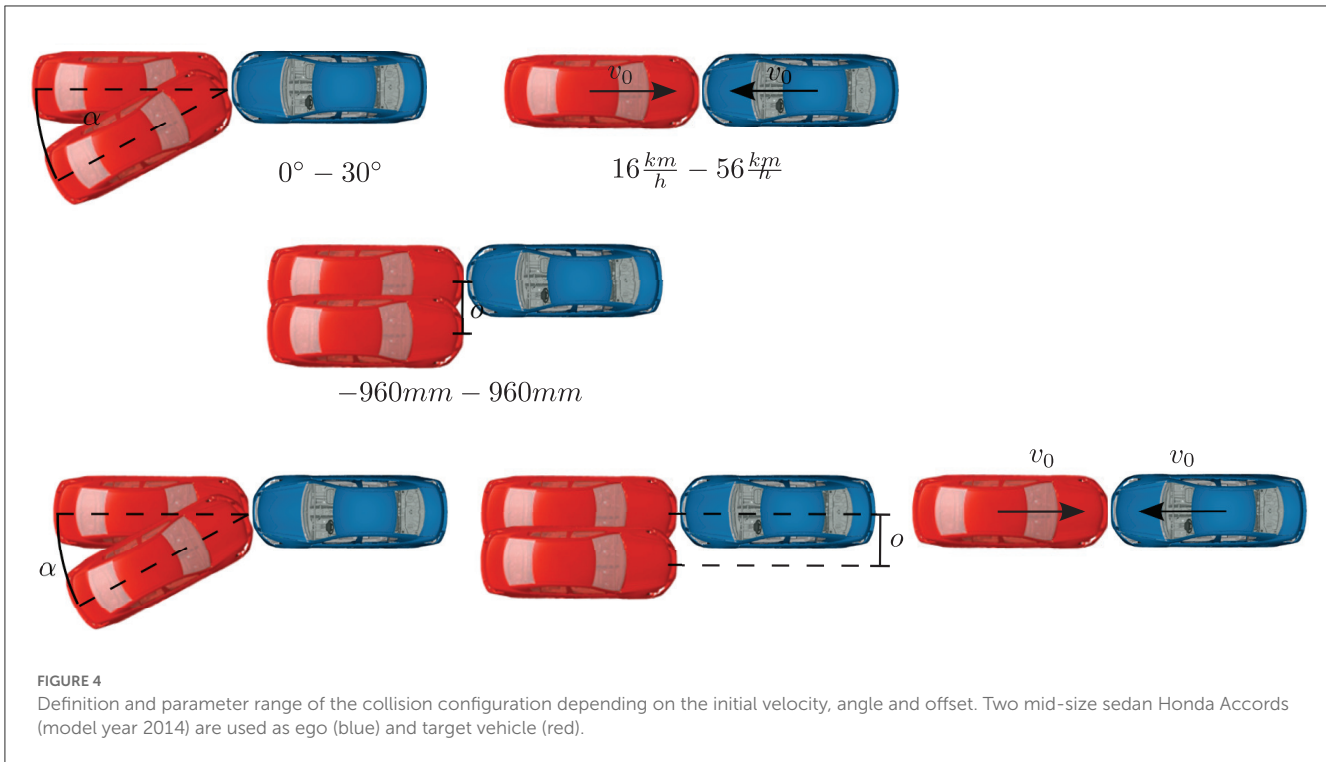
The training data generation process involves multiple simulation steps that are illustrated in Figure 1. The simulation

framework consists of a scenario simulation, a vehicle crash simulation, and an occupant restraint system simulation that includes both the pre- and in-crash phase. A more in-depth explanation of the simulation framework is given in Wimmer et al. [10] and Hay [16].

The generation process of synthetic driving and collision scenarios (Figure 2Ba) involves two conflict partners, sampling of different parameter distributions (e.g. velocity, acceleration, steering angle), which are constrained to physical limits, and includes a CarMaker vehicle dynamics model. The generated scenarios are then filtered so that only the remaining 285 driving scenarios resulting in the configuration in Figure 4 are considered as baseline for the restraint system parameter optimization.

The scenario simulation (Figure 2Ba) provides vehicle trajectories with corresponding accelerations  $a_v \in [0, t_0]$ , that are transferred to the occupant restraint system simulation. In addition, the last time step of the scenario simulation describes the collision configuration in dependence of the initial velocity, the angle and offset of the target and ego vehicle. The parameters describing the collision configuration were chosen such that the results are bound by a subset of all possible configurations in the scenario simulation results, which are limited to the indicated configuration ranges in Figure 4. The impact angle is chosen within the range of common frontal barrier crash tests.

The collision configuration defines the initial condition of the vehicle to vehicle crash simulation (Figure 2Bb), which is performed in LS-Dyna (Version 9.2) with two Honda Accord models [17]. In order to reduce the complexity in this initial proof of concept only one vehicle type without a variation of the mass is considered. A vehicle crash FEM simulation however requires large computational efforts and results in simulation times of more than 20 h. To be able to consider a broad variation of loading conditions in very short time frames, the surrogate model developed in [11] was used to approximate the crash pulse in an efficient way. The predicted crash pulses  $\mathbf{a}_p \in [t_0, t_{end}]$  are then appended to the pre-crash time signals  $\mathbf{a}_v$  and applied to a Madymo occupant restraint system simulation model (Figure 2Bc). The Madymo model consists of a vehicle interior, defined by multi-bodies and an FE instrument panel. The Madymo AHM (Version 3.1) is positioned on the driver seat and a FE three-point-belt with bar elements between d-ring



and buckle is attached, see Figure 5. Furthermore, a generic and scalable driver airbag with a volume of approximately 40 l is installed.

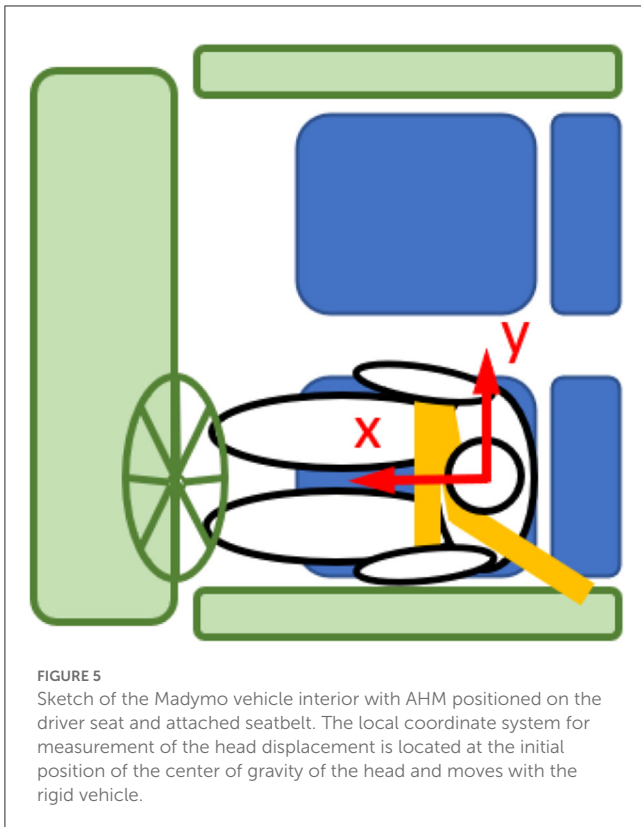
The model allows a modification of restraint system parameters  $\mathbf{p}_{\text{Restraint}}$ , such as the airbag time to fire  $AB_{TFF}$ , the airbag vent diameter  $d_{\text{Vent}}$ , the retractor pretensioner load limiter  $PT_U$  and the retractor pretensioner time to fire  $PT_{TFF}$ . The occupant restraint system simulation is performed with Madymo Version 7.8.

During the simulation, the relative head displacement  $\mathbf{d}_{\text{head}}^{PC} = \{head_x, head_y\}$  is measured, see Figure 6, and used as representation of the occupant’s seating position resulting from the pre-crash scenario. The head position is chosen since a displacement of the head is likely to result in a variation of the point of impact on the airbag and potentially in a higher probability of sliding alongside the airbag, contact with the vehicle interior and increased injury probability. However, the occupant motion and head trajectory depend on the pre-crash acceleration  $a_v$ . Since the generation of acceleration signals that result in specific head positions is nontrivial, the available pre-crash acceleration signals were analyzed and nine grid-like samples that cover the range of motion were selected for training data generation (see Figure 6). The selected pre-crash scenarios include maximum longitudinal decelerations of  $8.5 \frac{m}{s^2}$  and maximum lateral accelerations of  $4.5 \frac{m}{s^2}$  and are therefore presumed to enclose the relevant parameter space. The surrogate model is then assumed to learn the correlation between the training samples for all head positions in the defined range in order to predict the respective AHM response. Although the Madymo simulation provides multiple

injury criteria, this study only focuses on the  $HIC_{36}$  and chest deflection.

For each sampling method Madymo simulations are performed based on the nine selected pre-crash accelerations and crash pulses resulting from collision configurations in the range of Figure 4. In addition, a variation of the restraint system parameters is performed. The retractor pretensioner load limiter, the airbag vent diameter and the airbag and retractor pretensioner time to fire (ttf) are each varied around a standard setup without considering the current technical limitations to a full extent. The training data set then consists of a combination of the input parameter in Table 1 and the corresponding  $HIC_{36}$  and chest deflection values for each simulation.

The prediction framework, including the trained surrogate model is illustrated in Figure 3. For each scenario, a simulation of the occupant movement in the pre-crash phase is required to determine the head position at the time of collision. A computational efficient approximation of the occupant movement is achieved by usage of a simplified physics-based occupant model that is similar to the one described in Cyrén and Johansson [18]. The surrogate model will then predict  $\mathbf{y} = \{HIC_{36}, CD\} \in \mathbb{R}^2$ , i.e., the head injury criterion ( $HIC_{36}$ ) and chest deflection (CD) for given  $\mathbf{X}$ , i.e., the initial head position  $\mathbf{d}_{\text{head}}^{PC}$ , the collision configuration  $\mathbf{p}_{\text{Collision}}$ , and a chosen set of restraint system parameters  $\mathbf{p}_{\text{Restraint}}$ . In vehicle safety simulations, injury values can vary greatly, with very high injury values resulting, for example, from low airbag pressure or a displaced impact position and thus contact with the steering wheel or vehicle interior. Since state-of-the-art restraint systems are only designed and optimized

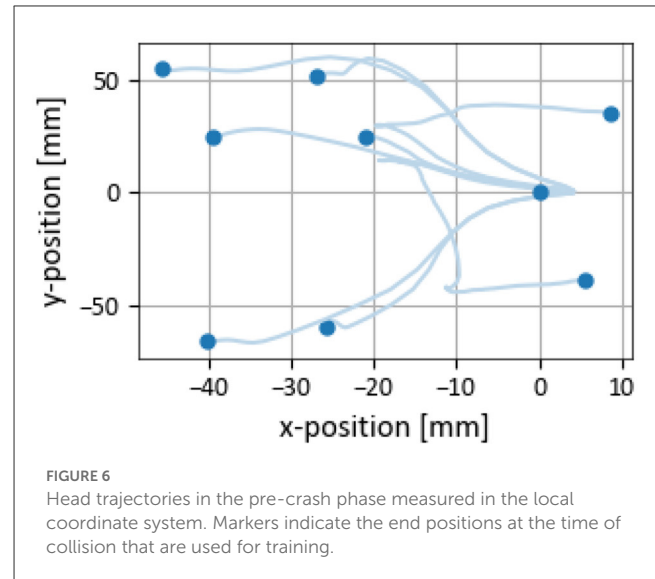


for standard load-cases, discontinuities and high injury values, especially in the marginal area, may therefore occur during scenario-based tests. With the help of the proposed surrogate modeling method, the limits of current safety technologies can be demonstrated and new concepts for better protection of vehicle occupants can be developed.

## 2.2. Sampling methods

Mathematical surrogate models solely rely on the quality of the input data  $X$  and output data  $Y$ . In engineering, the training data is either available from prior simulation or experimental results or has to be generated only for surrogate modeling purposes. In this study, simulation for machine learning is done, i.e., a Madymo simulation with a computation time of  $\sim 2$  h is performed for each sample in the training set. The samples have to be chosen strategically to minimize the computational expenses for training data generation.

Design of experiments methods (see e.g., [19, 20]), aim at maximizing the information extracted from resource-constrained systems. Therefore, design of experiment methods are well suited to select the most suitable parameter combination to maximize the information extraction in the surrogate modeling process. The design of experiments offers a wide range of statistical sampling methods, which can be divided into static and adaptive methods. D-optimal design and space-filling design are static sampling methods that determine the sample distribution a-priori; a third sampling



method used in this publication, “Adaptive Sampling”, adapts the samples in an online step. A challenge in occupant simulations is that not all parameters are continuously adjustable. Thus, sampling methods that consider constraints and bounds need to be chosen, or existing methods need to be modified. As learning is new in occupant simulation the accuracy of the resulting surrogate models in dependence on the chosen sampling strategy is assessed using a test dataset.

### 2.2.1. D-optimal design

The d-optimal is a computer-aided design, which is well suited for constrained design spaces [21]. The optimization-based design maximizes the determinant  $D = |\mathbf{X}^T \mathbf{X}|$ , also known as information matrix, which is equal to minimizing the variance of the parameter estimates. A d-optimal design is thus not orthogonal, and correlations of the parameter estimates are possible. The chosen samples are mostly present at the edges of the parameter space, with only a few samples in the inner part. In this study, a d-optimal design with 100 samples was created in the commercial tool Cornerstone (Version 7.1).<sup>2</sup>

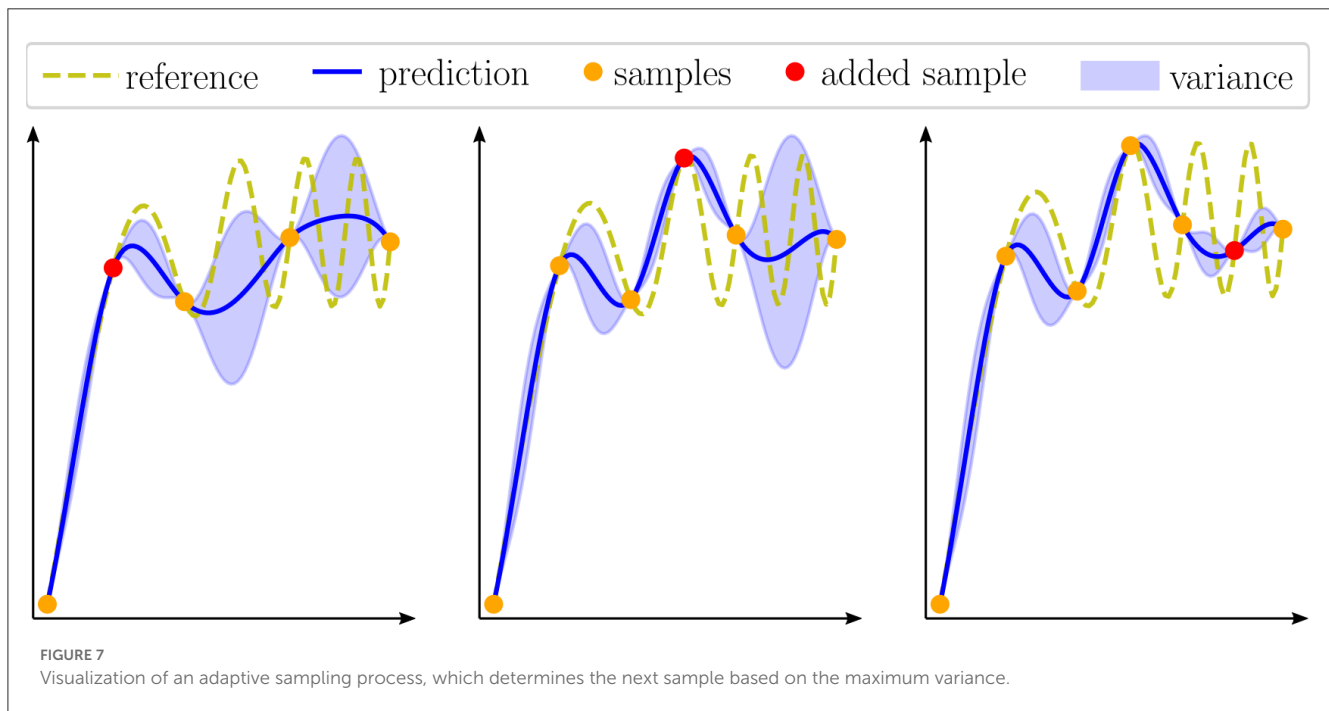
### 2.2.2. Space-filling design

Space-filling approaches, such as Latin Hypercubes, provide better coverage of the inner parameter space than d-optimal designs [22]. With higher dimensionality of a dataset, the probability of insignificant parameters is increasing. Thus, a space-filling design will yield a higher information gain with the same computational effort. Hence, surrogate models trained with a space-filling dataset are expected to make predictions with higher accuracy in the inner part of the parameter space than a model trained on d-optimal data. However, samples are less represented at the parameter

<sup>2</sup> <https://www.camline.com/products/cornerstone/>, accessed 2023/01/20.

TABLE 1 Considered input parameter ranges for human body model response prediction.

Pre-crash occupant position at $t_0$			Collision configuration at $t_0$			Restraint system parameter			
	Head Position x [mm]	Head Position y [mm]	Impact angle [°]	Offset [mm]	Initial velocity [km/h]	Airbag ttf [ms]	Vent diameter [mm]	Retractor pretensioner ttf [ms]	Retractor pretensioner load limiter [N]
Min	-45.7	-67.3	0	-960	27	5	35	5	3,500
Max	8.6	59.9	30	960	56	15	45	15	5,500



space edges, so the space-filling surrogate model might return more inaccurate extrapolations. A space-filling design, however, requires all parameters to be adjustable to all possible values in the chosen interval. Since only nine head positions are used for training, see Section 2.1 “Simulation Framework for Training Data Generation”, the space-filling design has to be modified. Instead of using the head position calculated by the space-filling design, the Euclidian-norm measured nearest neighbor in the available positions in Figure 6 is selected. Two datasets with 100 samples each are generated with the space-filling design in Cornerstone, one for training and one for validation of the surrogate models.

### 2.2.3. Adaptive sampling

In contrast to statistical sampling methods, which determine the sample size and location in advance, an adaptive sampling scheme allows to sequentially sample the parameter space and take the surrogate model accuracy and prediction variance into account [23]. Surrogate models such as GPRs provide the variance—an estimate of the model’s accuracy— in addition to the prediction, so that the input parameter combination with the highest variance can be determined. Sampling iteratively at the points of maximum

variance, the model accuracy is increased until a termination criterion is reached, see the example in Figure 7.

Possible termination criteria include the maximum variance and the change in hyperparameters that are indicators for the model performance and under- or overfitting. A better choice for estimating the true model accuracy is the cross-validation error. Hence, in each iteration, a leave-one-out cross-validation is performed to approximate the prediction error. The adaptive sampling algorithm is implemented in python.

## 2.3. Gaussian process regression

A Gaussian process regression (GPR) is a Bayesian approach to regression which infers unseen data given a chosen prior distribution [24]. In comparison to other machine learning algorithms, Gaussian processes provide a variance in addition to the mean prediction, which can be thought of as an estimate of the model’s accuracy. Furthermore, GPRs are well suited for smaller datasets.

Assuming a zero mean, the joint multivariate prior for the training outputs  $y$  and test outputs  $f$  reads as

$$\begin{bmatrix} \mathbf{y} \\ \mathbf{f}_* \end{bmatrix} \sim \mathcal{N} \left( \begin{bmatrix} 0 \\ 0 \end{bmatrix}, \begin{bmatrix} \mathbf{K}(\mathbf{X}, \mathbf{X}) + \sigma_n^2 \mathbf{I} & \mathbf{K}(\mathbf{X}, \mathbf{X}_*) \\ \mathbf{K}(\mathbf{X}_*, \mathbf{X}) & \mathbf{K}(\mathbf{X}_*, \mathbf{X}_*) \end{bmatrix} \right), \quad (1)$$

with the training inputs  $\mathbf{X}$ , noise  $\sigma_n^2$ , test inputs  $\mathbf{X}_*$  and the covariance function or kernel  $K$ . With  $\sigma_n^2 = 0$  the GPR predictions will pass through all samples. Notice that most of the information is embedded in the kernel  $K$ . Therefore, the selection of the kernel has major influences on the accuracy of a gaussian process. Two popular choices of the kernel are the squared exponential (SE) and Matern kernel

$$\mathbf{K}_{SE}(\mathbf{x}, \mathbf{x}') = \exp \left( -\frac{d(\mathbf{x}, \mathbf{x}')}{2l^2} \right) \quad (2)$$

$$\mathbf{K}_{Matern}(\mathbf{x}, \mathbf{x}') = \frac{2^{1-\nu}}{\Gamma(\nu)} \left( \frac{\sqrt{2\nu}d(\mathbf{x}, \mathbf{x}')}{l} \right)^2 K_\nu \left( \frac{\sqrt{2\nu}d(\mathbf{x}, \mathbf{x}')}{l} \right) \quad (3)$$

with the length scale  $l$ , the Euclidean distance  $d$ , the gamma function  $\Gamma$  and the modified Bessel function  $K_\nu$ . The parameter  $\nu$  controls the function's smoothness so that for  $\nu \rightarrow \infty$  the Matern kernel converges to the squared exponential kernel. During training, the kernel parameters are optimized by minimizing the negative log-likelihood

$$\log p(\mathbf{y}|\mathbf{X}) = -\frac{1}{2} \mathbf{y}^T (\mathbf{K} + \sigma_n^2 \mathbf{I})^{-1} \mathbf{y} - \frac{1}{2} \log |\mathbf{K} + \sigma_n^2 \mathbf{I}| - \frac{n}{2} \log 2\pi, \quad (4)$$

with the number of samples  $n$ . Finally, with equation (1) the conditional joint posterior distribution is then computed as

$$\mathbf{f}_* | \mathbf{X}, \mathbf{y}, \mathbf{X}_* \sim \mathcal{N}(\bar{\mathbf{f}}_*, \text{cov}(\bar{\mathbf{f}}_*)), \quad (5)$$

$$\bar{\mathbf{f}}_* = \mathbf{K}(\mathbf{X}_*, \mathbf{X}) [\mathbf{K}(\mathbf{X}, \mathbf{X}) + \sigma_n^2 \mathbf{I}]^{-1} \mathbf{y} \quad (6)$$

$$\text{cov}(\bar{\mathbf{f}}_*) = \mathbf{K}(\mathbf{X}_*, \mathbf{X}_*) [\mathbf{K}(\mathbf{X}, \mathbf{X}) + \sigma_n^2 \mathbf{I}]^{-1} \mathbf{K}(\mathbf{X}, \mathbf{X}_*) \quad (7)$$

The covariance can later be used to assess the model quality or generate new training samples in regions with higher model uncertainty [25].

### 2.4. Surrogate model training process

In order to develop a surrogate model for occupant safety system simulations, training data is generated with the Madymo AHM for all three sampling methods. Subsequently, a GPR is trained on each of the training datasets consisting of the input data in Table 1 and the corresponding HIC<sub>36</sub> and chest deflection as output. The chest deflection is assumed to be smoothly distributed over the entire parameter range and thus, a squared exponential kernel is chosen for constructing the GPR. The HIC<sub>36</sub> response surface is however believed to have a rougher shape, due to nonlinearities resulting from airbag and steering wheel contact. Thus, a Matern kernel is used to model the HIC<sub>36</sub> response. After

TABLE 2 Training and joint test data sets.

Training data	Joint test data
d-optimal	Space filling, adaptive sampling, test set
Space filling	d-optimal, adaptive sampling, test set
Adaptive sampling	d-optimal, space filling, test set

training, all surrogate models are validated on the test set which contains 100 space-filling samples. In order to assess the model quality in a more general and sampling method independent way, all the samples that were not used for training are added to the test dataset, which results in the training and joint test sets in Table 2.

The accuracy of the surrogate models is then assessed using the mean absolute error (MAE) and coefficient of determination (R2 score). By analyzing the kernel hyperparameters and the shape of the response surface overfitting is evaluated.

### 2.5. Restraint system optimization

The best performing model is later applied for an optimization of the restraint system parameters. Since the objective function should reduce the combined AIS2+ injury risk for HIC<sub>36</sub> and chest deflection, first the individual injury risks [26] are computed as

$$P_{Head,AIS2+} = \mathcal{N} \left( \frac{\ln(HIC_{36}) - 6.96352}{0.846664} \right), \quad (8)$$

$$P_{Thorax,AIS2+} = \mathcal{N} \left( \frac{1}{1 + e^{(1.8107 - 0.4439 * D_{max})}} \right). \quad (9)$$

A joint injury risk [27] can then be calculated with

$$P_{joint,AIS2+} = P_{Head,AIS2+} + P_{Thorax,AIS2+} - (P_{Head,AIS2+} \times P_{Thorax,AIS2+}). \quad (10)$$

To find the optimal restraint system configuration that best protects the occupant, an optimizer is used to minimize the AIS2+ injury risk for each given collision scenario. Since surrogate model are used to approximate the injury risk, an optimizer that is not gradient-based and can handle discontinuities is required. Thus, the differential evolution algorithm [28], a global optimizer, is used in this work.

First an objective function  $f$  is defined. Then the following algorithm is performed.

Generate initial population  $x$  of size  $n$

While not termination criterion

For  $j = 1:n$

Generate three random integers  $i_1, i_2, i_3 \in (1, n)$  with

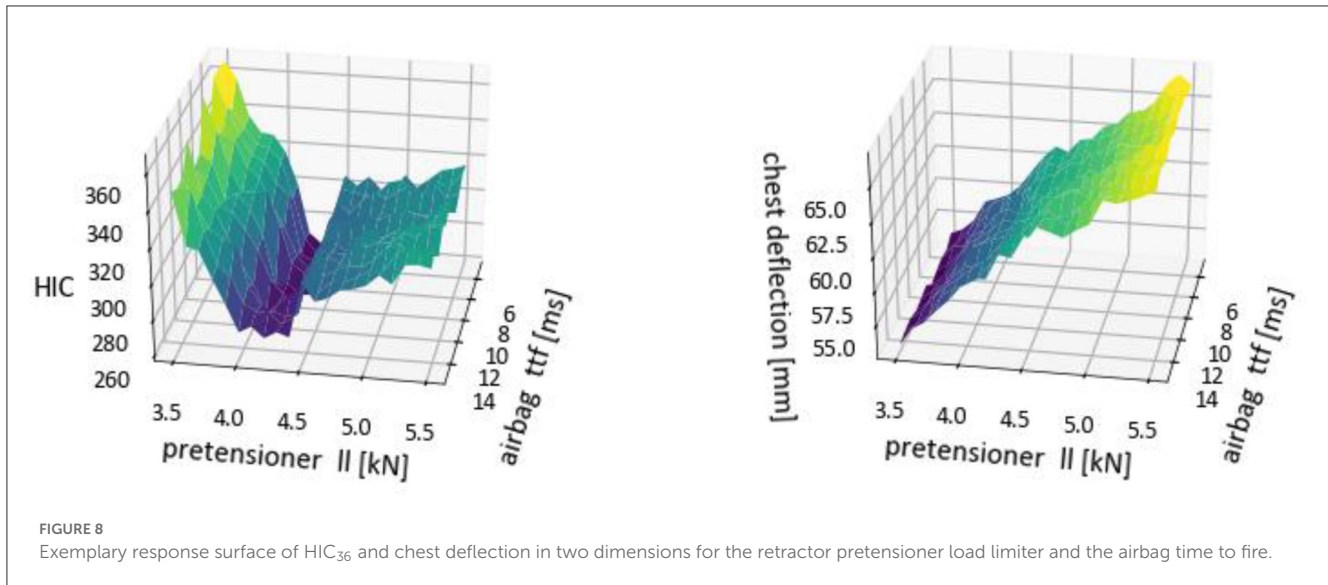
$i_1 \neq i_2 \neq i_3 \neq k$

Generate random integer  $i_{rand} \in (1, n)$

For  $k = 1:n\_parameter$

$$x'_{j,k} = \begin{cases} x_{j,i_3} + F^*(x_{j,i_3}, x_{j,i_1}, x_{j,i_2}) & \text{if } \text{rand}(0,1) < CR \text{ or } i = i_{rand} \\ x_{j,k} & \end{cases}$$

$x_j = x'_j$  if  $f(x_j) \geq f(x'_j)$



with the crossover probability  $CR$  and the differential weight  $F$ . Typical settings are  $CR = 0.9$  and  $F = 0.8$ .

### 3. Results

Before generating the entire training dataset, a two-dimensional subset of the parameter space, consisting of the retractor pretensioner load limiter and the airbag time to fire, was densely sampled to get an understanding of the resulting response surfaces. In [Figure 8](#) the response surfaces of  $HIC_{36}$  and chest deflection are shown over the retractor pretensioner load limiter ( $II$ ) and the airbag time to fire. The response surface of the  $HIC_{36}$  is rougher and nonlinear in comparison to the smooth response surface of the chest deflection. This justifies the different kernel choice for modeling the  $HIC_{36}$  and chest deflection distribution.

Subsequently, the sampling methods are used for training data generation. As expected, the d-optimal design samples mostly at the edges, whereas the space-filling design covers the entire parameter space (see [Figure 9](#), [Appendix 1](#)).

The adaptive sampling strategy on the other hand, chooses its next sample based on the variance of the GPR prediction, which continuously increases with the distance to given samples. Thus, an adaptive sampling algorithm will start to sample the edges before covering the inner part of the parameter space. A nine-dimensional parameter space with  $2^9$  vertices will thus cause the algorithm to sample at the edges almost exclusively for the first few hundred simulations. The adaptive sampling algorithm was aborted after 500 simulations, as the ratio of computational effort to prediction accuracy didn't significantly improve. The difference in the response surface of  $HIC_{36}$  and chest deflection is also reflecting in the error curve in [Figure 10](#). During the first 50 iterations the chest deflection MAE is already reduced to a low value and is slightly decreasing in the remaining iterations. The rougher shape of the  $HIC_{36}$  response surface however requires a more significant number of samples to reach the desired accuracy.

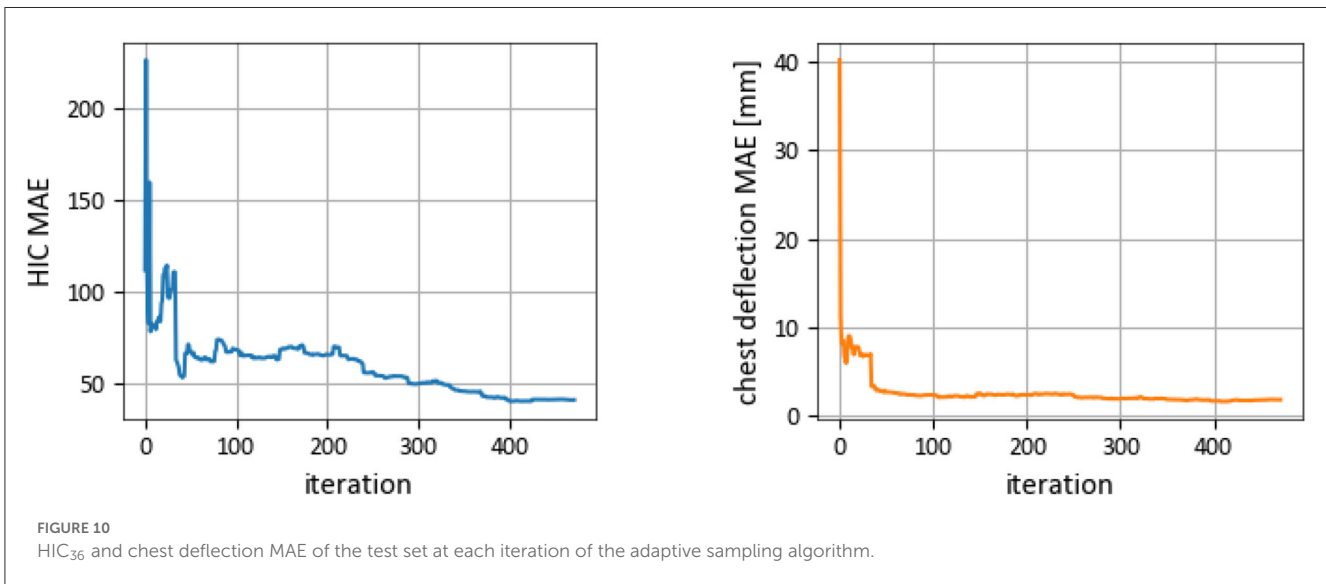
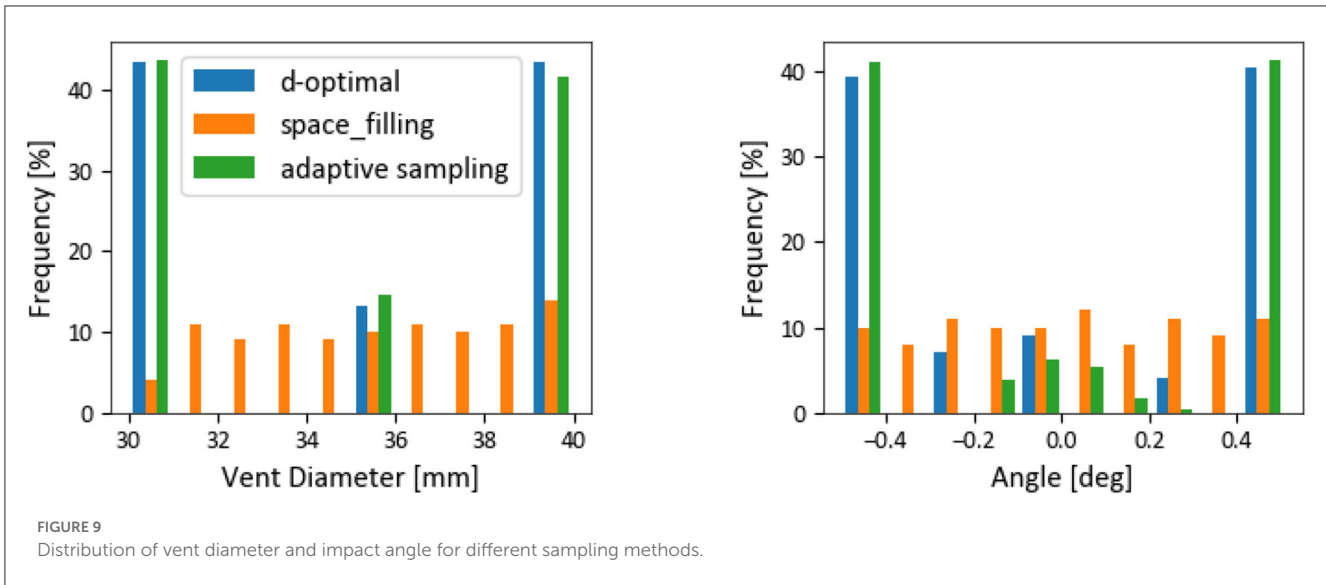
The three datasets that are generated with a d-optimal, space-filling and adaptive sampling, result in different distributions of the  $HIC_{36}$  and chest deflection (see [Figure 11](#)).

The majority of the  $HIC_{36}$  values are allocated in a range below 750. [Figure 11](#) suggests that high  $HIC_{36}$  values only occur at the edges of the input parameter space, as no  $HIC_{36}$  values above 500 are observable in the space-filling dataset and only the d-optimal design shows  $HIC_{36}$  values up to 1,800. As the adaptive sampling algorithm chooses the first samples primarily at the edges of the parameter space, the adaptive sampling dataset also includes a few samples with larger  $HIC_{36}$  values. The chest deflection on the other hand is well distributed over the entire domain, where only the d-optimal data set shows very small values.

#### 3.1. Surrogate model performance

A GPR is trained on each of the d-optimal, space-filling and adaptive sampling datasets and validated on the test sets in [Table 2](#). For zero noise the GPR predictions will go through every given sample in the training set. Therefore, the analysis of the predicted results focuses on the test data. Overfitting can still be excluded as the lengthscales of the surrogate model are each in a moderate range around 1 [24], which results in a smooth response surface (see [Appendix 2](#)). [Figure 12](#) shows the prediction of  $HIC_{36}$  and chest deflection over the test data. The red line represents identical prediction and simulation results. In general, all surrogate models are able to predict the chest deflection values in the entire range with higher accuracy, while the  $HIC_{36}$  predictions are only accurate in the lower range. Since only the d-optimal design data incorporates very large  $HIC_{36}$  values and low chest deflections, the GPR trained on the d-optimal dataset tends to overshoot the  $HIC_{36}$  and underestimate the chest deflection values.

Both the models trained on the space-filling and adaptive sampling dataset predict  $HIC_{36}$  and chest deflection with higher accuracy, resulting in smaller MAE and larger  $R^2$  score (see



Tables 3, 4). The model trained on the space-filling set shows a larger error on the d-optimal and adaptive sampling set, which contain more samples at the edges of the parameter space and HIC values in a wider range. However, it performs well on the test set. The model trained on the adaptive sampling set shows the best and most robust performance on all test sets (see Appendix 4).

The surrogate model reduces test data computation time from the order of hours with Madymo to milliseconds for predicting HIC<sub>36</sub> and chest deflection.

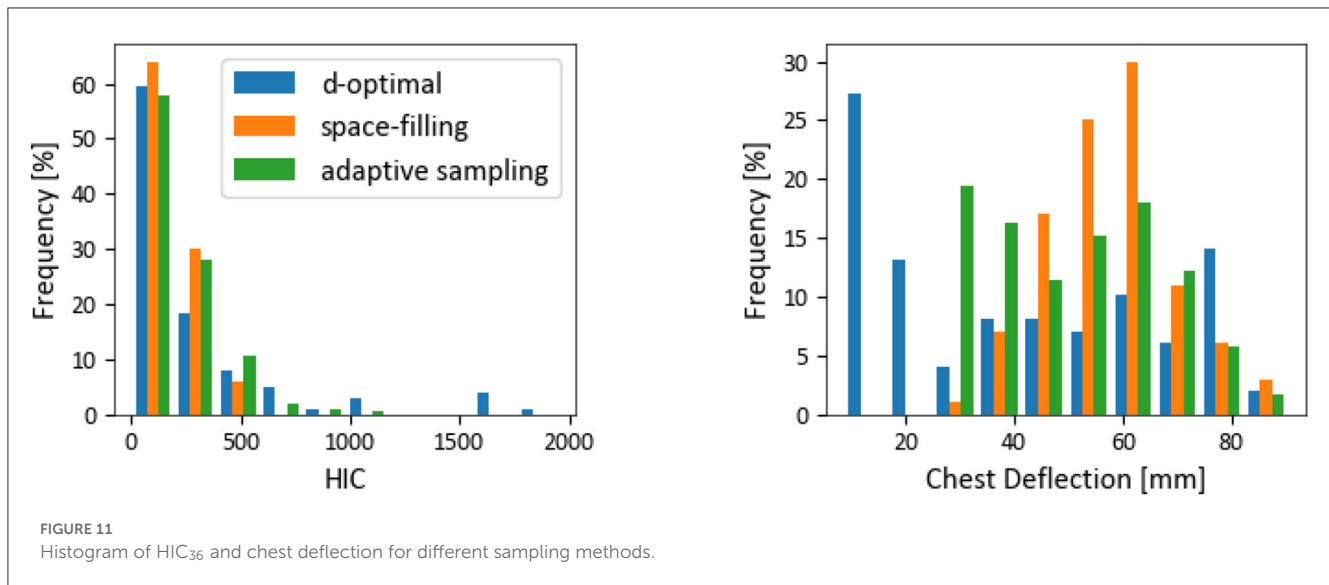
### 3.2. Restraint system optimization

Once efficient surrogate models are available it is possible to optimize the restraint system parameters individually for all 285 collision scenarios. For a given head position and collision scenario a differential evolution algorithm uses the injury value predictions by the GPR to find the optimal restraint system parameter

configuration that minimizes the joint AIS2+ injury risk for the given load-case. A convergence plot of the differential evolution algorithm is shown in Figure 12A. On average, 30 iterations are needed to find the optimal restraint system configuration. Thus, with a population size of 50, an average of 1,500 evaluations are performed per load case. This is only possible with the help of time-efficient surrogate models. Due to the fast prediction of injury values, an optimization is possible in  $0.9973 \pm 0.2976$  s. The predicted injury risk distribution before and after the optimization is illustrated in Figure 13.

For all trajectories and collision scenarios the joint AIS2+ injury risk can be reduced by 4% in average. The analysis of the optimized restrained system parameter showed no direct correlation to the input parameter, so a categorical adaptation of the restraint system for specific parameter regions does not make sense.

As the overall simulation process includes multiple FEM and MBS simulations the computation of high-fidelity results is rather expensive. Therefore, only a subset of the available scenarios, which



showed the largest injury risk reduction, was chosen for validation of the optimization results. As illustrated in Figure 14 the joint AIS 2+ injury risk computed with the surrogate model predictions mostly shows lower values than the simulation. However, the surrogate model manages to capture the overall relations and is able to find minima in the predicted response surface that correlate with the high-fidelity FEM and MBS simulation.

## 4. Discussion

In this study, a surrogate model for predicting the human body model response in frontal collisions was developed. In comparison to [13–15] the developed surrogate model approximates the HIC<sub>36</sub> and chest deflection of the driver based on the occupant's head position resulting from pre-crash movement, the collision configuration and selected restraint system parameters. Furthermore, the developed surrogate model was used for a subsequent optimization of the restraint system parameters. The surrogate model was trained on simulations with a Madymo AHM, which is considered the baseline. Therefore, the model accuracy is not expected to surpass the accuracy of the Madymo simulation model.

The main focus of this study was the assessment of different sampling strategies to address the tradeoff between computational effort for training data generation and resulting surrogate model accuracy. Overall, the models trained on the d-optimal, space-filling and adaptive sampling dataset performed well in predicting the chest deflection, which has a smooth response surface (see Figure 8).

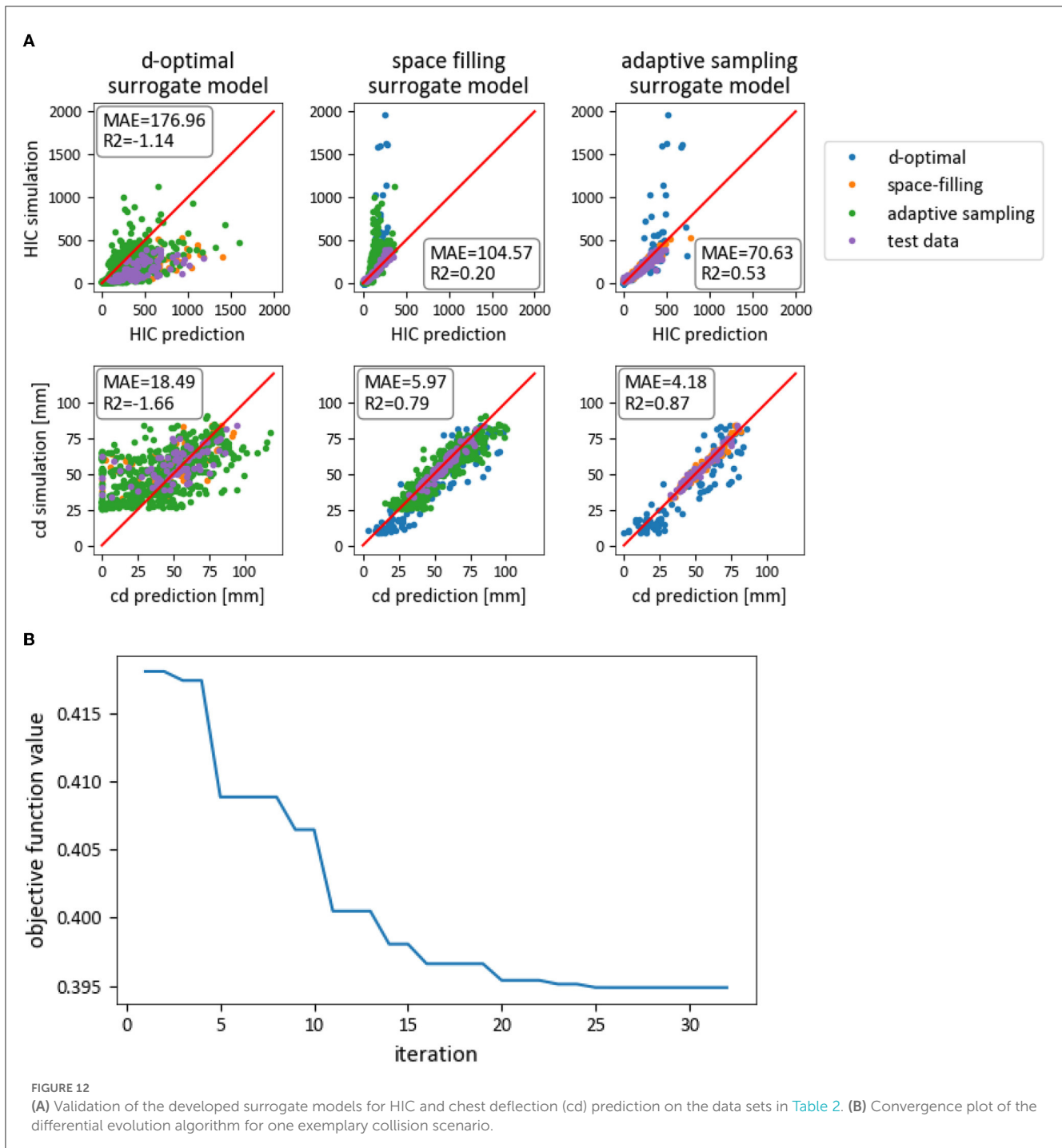
The model trained on the d-optimal dataset shows the lowest accuracy on all test sets (see Table 3). Due to a large number of samples at the edges of the parameter space (see Figure 9), the d-optimal model is not able to accurately interpolate in the inner part of the parameter space.

The prediction of the HIC<sub>36</sub> is less accurate, especially in the region of high HIC<sub>36</sub> values (see Figure 12). These high HIC<sub>36</sub> values occur at the edges of the parameter space, leading to an extrapolation of the surrogate models. The high injury values can be explained by the variation of the restraint system parameters, since, for example, as shown in Figure 8, a low seat belt load limit (pretensioner II) causes a severe impact on the airbag and a direct contact with the steering wheel, while a too high limit restrains the occupant too tightly to the seat and thus causes moderate head accelerations and a high chest deflection.

The model based on the space-filling strategy provides the chest deflection with an acceptable accuracy but fails to predict a HIC<sub>36</sub> larger than 500 (see Figure 12), as the space-filling training set does not contain any larger values, as shown in Figure 11. Since the training set is well distributed in the entire parameter space, the model is able to accurately interpolate in the desired range. All large HIC<sub>36</sub> values are distributed at the edges of the parameter space and thus only present in the d-optimal and partially in the adaptive sampling data set (see Figure 11).

Therefore, the adaptive sampling model performs better on the test datasets. However, the prediction of large HIC<sub>36</sub> values is not sufficiently accurate. Furthermore, the creation of the adaptive sampling data set required five times more simulations than the d-optimal and space-filling design.

One drawback of the developed surrogate models is the low accuracy in the higher HIC<sub>36</sub> range, which are mostly occurring at the edges of the parameter space and are underrepresented in all training sets. By generating more samples with high HIC<sub>36</sub> values, the model accuracy could be improved in this range. As the correlation between input parameter and injury values is unknown, this task is expected to be challenging. One possible solution could be the application of an adaptive sampling algorithm with the objective of maximizing the HIC<sub>36</sub>.



Without an accurate prediction of the entire HIC<sub>36</sub> range, a valid prediction range in the parameter space must be defined to apply the model for quantitative safety critical analysis. An a priori classification of the HIC<sub>36</sub> range and training of a second model for large HIC<sub>36</sub> values might be possible.

For qualitative analyses considering the inner part of the parameter range the accuracy of the developed surrogate model appears to be sufficient, so that the model can be applied for injury value prediction and restraint system optimization. The developed surrogate model is able to approximate the

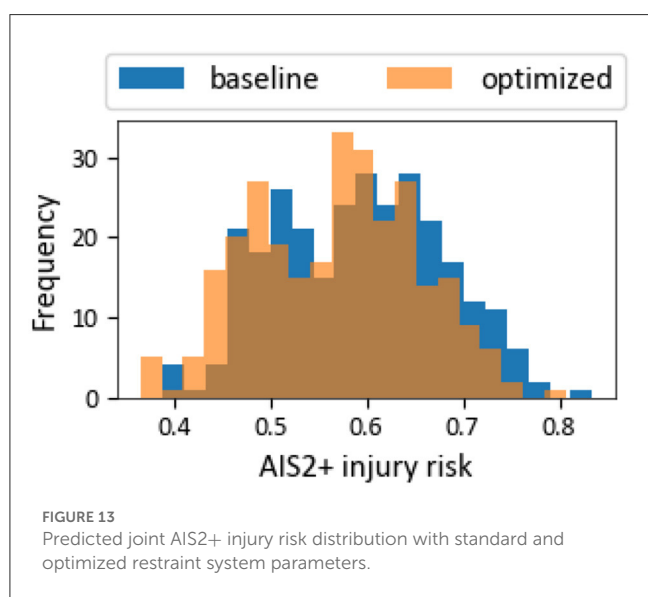
HIC<sub>36</sub> and chest deflection with a computation time reduction of roughly 99% compared to a simulation with the Madymo AHM. With the reduced computation time the surrogate model enables large scale scenario-based assessment of vehicle safety systems. In addition, the surrogate model allows an efficient optimization of the restraint system for a given collision scenario and thus a reduction of the resulting joint AIS2+ injury risk. The comparison of the predicted and optimized joint AIS2+ risk with the FEM and Madymo results showed that the surrogate model manages to capture the basic trends and reduces the joint AIS2+ injury risk in the validation

TABLE 3 HIC<sub>36</sub> mae of the trained models on the available datasets.

	d-optimal set	Space-filling set	Adaptive sampling set	Test set	Joint set
d-optimal	0	286.10	136.81	271.97	284.82
Space filling	186.58	0	101.83	23.97	104.57
Adaptive sampling	133.14	34.94	0	39.80	70.63

TABLE 4 Chest deflection mae of the trained models on the available datasets [mm].

	d-optimal set	Space-filling set	Adaptive sampling set	Test set	Joint set
d-optimal	0	12.52	20.78	12.77	18.49
Space filling	9.60	0	5.85	2.38	5.97
Adaptive sampling	8.53	1.97	0	1.72	4.18



simulations, even though the predicted injury values deviate from the actual values.

### 4.1. Limitation of the study

One drawback of the developed surrogate models is the low accuracy in the higher HIC<sub>36</sub> range, which are mostly occurring at the edges of the parameter space and are underrepresented in all training sets. By generating more samples with high HIC<sub>36</sub> values, the model accuracy could be improved in this range. As the correlation between input parameter and injury values is unknown, this task is expected to be challenging. One possible solution could be the application of an adaptive sampling algorithm / active learning techniques with the objective of maximizing the HIC<sub>36</sub>. For d-optimal sampling further research is required to assess whether an increased sample size in a d-optimal sense could improve the model performance.

If a higher accuracy of the training set is desired, the entire process can be repeated with a more detailed occupant model, i.e., a finite element model. Then, however, the computation

time for training data generation would increase tremendously. In addition, the surrogate model is only valid for the chosen restraint system, vehicle type and occupant –the training data and result prediction was on the 50% AHM with a restraint system consisting of fixed components, i.e., one airbag and one retractor pretensioner. For a broad-scale application of the presented method, the sensitivity of the surrogate models to different occupant sizes (starting from 5% and 95% parameters should be investigated, in combination with varied restraint systems components and parameters. So far any change in the vehicle structure or restraint system configuration, e.g., new type of airbag, new training of the surrogate model is required.

To date, only pairwise evaluations of the forecasted and optimized combined AIS2+ risk have been conducted. In a further study the optimization of the safety system should be performed with a high-fidelity model or a multifidelity method [29]. R2 values for HIC and chest deflection prediction are presented in the Tables 5, 6 for all available datasets.

## 5. Conclusion

As driver assistance systems and autonomous vehicles become more prevalent, the safety systems in vehicles are becoming increasingly intricate. This complexity offers the potential to enhance occupant safety by utilizing sensor data from active safety systems to adjust passive safety components. To effectively evaluate the performance of these integrated safety systems, it is necessary to consider all relevant load cases. Scenario-based methods are required to achieve a comprehensive evaluation. The resulting insights can inform strategic decisions and enable early product placement during development.

Overall, reducing the computational cost of simulating integrated vehicle safety systems will be an important area of research in the future, as it will enable researchers and engineers to evaluate all relevant load cases. Crash simulations often involve large amounts of data, which can be difficult to process and analyze. Therefore, one challenge and the main topic of this work was providing the data in such a format that the data-based MOR method could efficiently work with the data, and we can compare which sampling strategy is most suited for crash

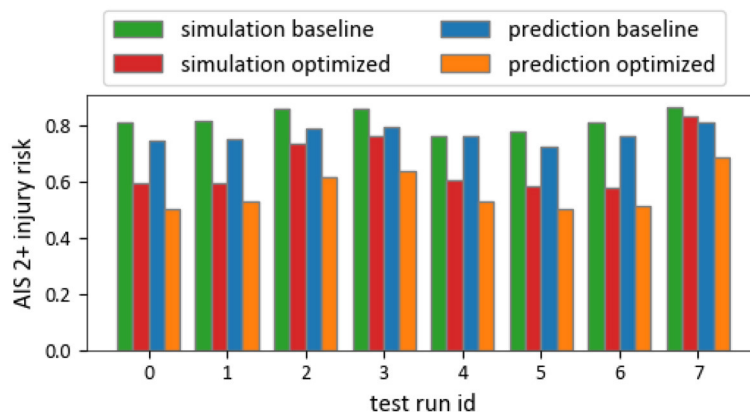


FIGURE 14 Comparison of prediction and simulation results with and without optimized restraint system parameter for a selected subset of the available scenarios.

TABLE 5 HIC<sub>36</sub> R2 score of the trained models on the available datasets.

	d-optimal set	Space-filling set	Adaptive sampling set	Test set	Joint set
d-optimal	1	-8.55	-0.16	-8.74	-1.14
Space filling	0.10	1	0.23	0.89	0.2
Adaptive sampling	0.47	0.83	1	0.75	0.53

TABLE 6 Chest deflection R2 score of the trained models on the available datasets.

	d-optimal set	Space-filling set	Adaptive sampling set	Test set	Joint set
d-optimal	1	-1.62	-1.79	-1.70	-1.66
Space filling	0.77	1	0.77	0.93	0.79
Adaptive sampling	0.81	0.95	1	0.96	0.87

simulations to gain the maximum out of the minimum amount of simulation.

In this study, the space-filling design provides the highest information gain and accuracy in relation to the number of samples and should be preferred for future applications. The adaptive sampling method then offers the possibility to further increase the prediction accuracy if computational resources are available.

As we have seen, the space-filling design provides the highest information gain and accuracy to the number of samples and should be preferred for future applications.

As we have seen, data-based MOR could be challenging for crash simulation because the model's response can jump once we leave the intended mode of operation of the safety system. Therefore, active learning approaches to find those critical modes of operation are worth further research.

The developed surrogate models provide only qualitative insights; if highly accurate results are required, a thorough assessment or validation with high-fidelity simulations must be performed. Comprehensive computer-based experiments and workflows must include surrogates in the development loop. Once the surrogates are part of the workflow, they should be permanently

monitored and retrained using all available data in the automotive industry. Hence, it is imperative to invest in efficient workflow technologies for labeling and accessing vast amounts of information to ensure a good and effective workflow with surrogate models in the future.

### Data availability statement

The datasets presented in this article are not readily available because the data can only be shared by consent of every author of article. Please contact the corresponding author. Requests to access the datasets should be directed to JF, [joerg.fehr@itm.uni-stuttgart.de](mailto:joerg.fehr@itm.uni-stuttgart.de).

### Author contributions

JH contributed to the research of suitable sampling methods, the development of surrogate models, and the overall analysis and evaluation. As project lead, LS enabled this research work and contributed with the general idea and expertise on the

overall process and methods for assessment of integrated safety systems. EB contributed to the design and build-up of the required restraint system configurations and with expertise to the AHM simulations and evaluations. PW contributed to the research and implementation of sampling methods and provided valuable feedback and expertise on surrogate modeling and assessment. OZ contributed to the setup of the FE simulations and the setup, assessment of Madymo simulations, and expertise according injury assessment and restraint systems. SK supported this research work and contributed with his expertise on assessment methods for the overall process for integrated safety systems. JF supervised JH in his research, contributed to the writing of the paper, citations of previous works, and the logical graphical presentation of the results. His revisions and important input improved the publication. All authors have read and approved the final manuscript.

## Funding

The publication was supported by Virtual Vehicle Research GmbH in Graz, Austria.

## Acknowledgments

The authors would like to acknowledge the financial support within the COMET K2 Competence Centers for Excellent Technologies from the Austrian Federal Ministry for Climate Action (BMK), the Austrian Federal Ministry for Digital and Economic Affairs (BMDW), the Province of Styria (Dept. 12), and the Styrian Business Promotion Agency (SFG). The

Austrian Research Promotion Agency (FFG) has been authorized for the programme management. We thank the Deutsche Forschungsgemeinschaft (DFG, German Research Foundation) for supporting this work by funding—EXC2075–390740016 under Germany's Excellence Strategy. We acknowledge the support by the Stuttgart Center for Simulation Science (SimTech).

## Conflict of interest

JH, LS, and EB are employed by ZF Friedrichshafen AG. PW, OZ, and SK are employed by Virtual Vehicle Research GmbH.

The remaining author declares that the research was conducted in the absence of any commercial or financial relationships that could be construed as a potential conflict of interest.

## Publisher's note

All claims expressed in this article are solely those of the authors and do not necessarily represent those of their affiliated organizations, or those of the publisher, the editors and the reviewers. Any product that may be evaluated in this article, or claim that may be made by its manufacturer, is not guaranteed or endorsed by the publisher.

## Supplementary material

The Supplementary Material for this article can be found online at: <https://www.frontiersin.org/articles/10.3389/fams.2023.1156785/full#supplementary-material>

## References

- European Commission. (2020). *European Commission: EU road safety policy framework 2021-2030 – Next steps towards "Vision Zero"*.
- Destatis. (2022). Available online at: <https://www.destatis.de/DE/Themen/Gesellschaft-Umwelt/Verkehrsunfaelle/Tabellen/liste-strassenverkehrsunaefalle.html> (accessed 15 February, 2022).
- Vollrath M, Schleicher S, Gelau C. The influence of cruise control and adaptive cruise control on driving behaviour a driving simulator study. *Accid Anal Prev.* (2011) 43:1134. doi: 10.1016/j.aap.2010.12.023
- Kelley WL. *Patent No. US4926171A, United States.* (1990).
- Grotz B, Straßburger P, Huf A, Roig L. Predictive safety - preception-based activation of pre-crash systems. *ATZ Worldwide.* (2021) 1:18–24. doi: 10.1007/s38311-020-0601-6
- OSCCAR23. *Future Occupant Safety for Crashes in Cars.* (2023). Available online at: <https://www.osccarproject.eu/> (accessed January 16, 2023).
- VIRTUAL23. Open access virtual testing protocols for enhanced road user safety, (2023). Available online at: <https://projectvirtual.eu/> (accessed January 16, 2023).
- Linder A. VIRTUAL-a European approach to foster the uptake of virtual testing in vehicle safety assessment. In: *8th Transport Research Arena TRA 2020.* Helsinki, Finland. (2020). Available online at: [https://projectvirtual.eu/wp-content/uploads/2020/03/VIRTUAL-TRA-2020-Linder-et-al\\_12Mar20.pdf](https://projectvirtual.eu/wp-content/uploads/2020/03/VIRTUAL-TRA-2020-Linder-et-al_12Mar20.pdf)
- Östh J, Larsson E, Jakobsson L. Human Body Model Muscle Activation Influence on Crash Response. In: *Proceedings of the IRCOBI Conference, IRC-22-101.* Porto, Portugal. (2022) p. 844–865.
- Wimmer P, Zehbe O, Kirschbichler S, Hay J, Schories L, Bayerschen E, et al. Surrogate Model Based Safety Performance Assessment of Integrated Vehicle Safety Systems. In: *NAFEMS World Congress, Online.* Glasgow: NAFEMS (2021).
- Hay J, Fehr J, Schories L. Crash Pulse Prediction for Scenario-based Vehicle Crash FE-Simulations. In: *Proceedings of the IRCOBI Conference, IRC-20-22.* Zürich: IRCOBI. p. 199–200. (2020).
- Reed MP, Ebert SM, D'Souza C, Jones ML. Predicting standing reach postures using deep neural networks. *Proc Hum Factors Ergon Soc Annu.* (2022) 66:662–666. doi: 10.1177/1071181322661150
- Joodaki H, Gepner B, Kerrigan J. Leveraging Machine Learning for Predicting Human Body Model Response in Restraint Design Simulations. In: *Computer Methods in Biomechanics and Biomedical Engineering,* 2020 doi: 10.1080/10255842.2020.1841754
- Bance I, Nie B. A Framework for near real-time occupant injury risk prediction using a sequence-to-sequence deep learning approach. In: *Proceedings of IRCOBI Conference, Florence.* Zürich: IRCOBI (2019).
- Berthelson PR, Ghassemi P, Wood JW, Stubblefield GG, Al-Graitti A, Jones M, et al. A finite element-guided mathematical surrogate modeling approach for assessing occupant injury trends across variations in simplified vehicular impact conditions. *Med Biol Eng Comput.* (2021) 59:1065–1079. doi: 10.1007/s11517-021-02349-3
- Hay J. A Surrogate Model-enhanced Simulation Framework for Safety Performance Assessment of Integrated Vehicle Safety Systems. In: *Dissertation, Schriften aus dem Institut für Technische und Numerische Mechanik der Universität Stuttgart, Vol. 75.* Aachen: Shaker Verlag. (2022).
- Singh H, Kan C-D, Marzougui D, Quong S. Update to future midsize lightweight vehicle findings in response to manufacturer review and IIHS small-overlap testing. *NHTSA* (Report No. DOT HS 812 237) (2016).
- Cyrén O, Johansson S. *Modeling of Occupant Kinematic Response in Pre-crash Maneuvers - A Simplified Human 3D-model for Simulation of Occupant Kinematics in Maneuvers.* Göteborg: Chalmers University of Technology. (2018).

19. Garud SS, Karimi IA, Kraft M. Design of computer experiments: a review. *Comput Chem Eng.* (2017) 106:71–95. doi: 10.1016/j.compchemeng.2017.05.010
20. Giunta A, Wojtkiewicz S, Eldred M. Overview of Modern Design of Experiments Methods for Computational Simulations (Invited). In: *41st Aerospace Sciences Meeting and Exhibit*. Reno (2012). doi: 10.2514/6.2003-649
21. Santner T, Williams B, Notz W. *The Design and Analysis of Computer Experiments*. Berlin, Germany: Springer. (2018) p. 145–152. doi: 10.1007/978-1-4939-8847-1\_5
22. Siebertz K, van Bebber D, Hochkirchen T. *Statistische Versuchsplanung*. Berlin, Germany: Springer. (2017) p. 55–56. doi: 10.1007/978-3-662-55743-3
23. Eason J, Cremaschi S. Adaptive sequential sampling for surrogate model generation with artificial neural networks. *Comp Chem Eng.* (2014) 68:220–32. doi: 10.1016/j.compchemeng.2014.05.021
24. Rasmussen C, Williams C. *Gaussian Processes for Machine Learning*. Cambridge, MA: MIT Press. (2006). doi: 10.7551/mitpress/3206.001.0001
25. Chen Y, Peng C. Intelligent adaptive sampling guided by Gaussian process inference. *Meas. Sci Technol.* (2017) 28:105005. doi: 10.1088/1361-6501/aa7d31
26. Eppinger R, Sun E, Bandak F, et al. *Development of Improved Injury Criteria for the Assessment of Advanced Automotive Restraint Systems-INHTSA I*. Washington, DC: National Highway Traffic Safety Administration (1999).
27. National Highway Traffic Safety Administration. *Consumer Information: New Car Assessment Program: Notice, Federal Register*. Washington, DC: National Highway Traffic Safety Administration (2008).
28. Storn R, Price K. Differential evolution - a simple and efficient heuristic for global optimization over continuous spaces. *J Global Optimizat.* (1997) 11:341–59 doi: 10.1023/A:1008202821328
29. Mäck M, Hanss M. Efficient possibilistic uncertainty analysis of a car crash scenario using a multi-fidelity approach. *ASCE-ASME.* (2018) 5:041015. doi: 10.1115/1.4044243